RSC Advances

This article can be cited before page numbers have been issued, to do this please use: S. mandal, D. sarkar, P. Rao, H. B. Aiyappa, S. Kurungot, S. Mandal and K. Ramanujam, *RSC Adv.*, 2016, DOI: 10.1039/C6RA05961A.

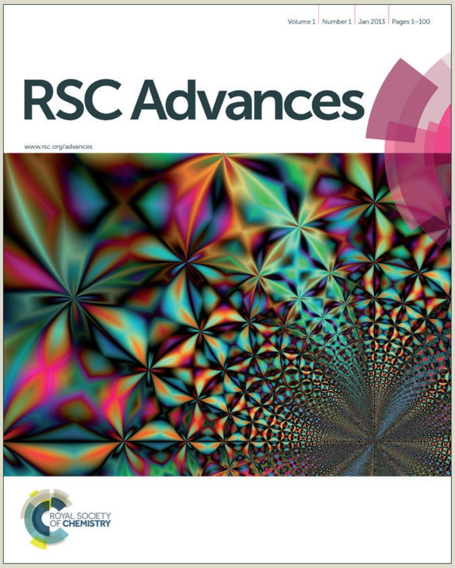

ROYAL SOCIETY OF CHEMISTRY

www.rsc.org/advances

View Article Online
DOI: 10.1039/C6RA05961A

Journal Name

RSCPublishing

ARTICLE

Cite this: DOI: 10.1039/x0xx00000x

Received 00th January 2012,
Accepted 00th January 2012

DOI: 10.1039/x0xx00000x

www.rsc.org/

Multifunctional Copper Dimer: Structure, Band Gap Energy, Catalysis, Magnetism, Oxygen Reduction Reaction and Proton Conductivity

Debraj Sarkar,[a] Purna Chandra Rao,[a] Harshitha Barike Aiyappa,[b,c] Sreekumar Kurungot,[b,c] Sudip Mandal,[d] Kothandaraman Ramanujam,[d] Sukhendu Mandal[a]*

A new dimeric copper complex namely, $[Cu_2(PDA)_2(Ald)_2(H_2O)_2]$. $8H_2O$, **1**, (where PDA = 2,4-pyridine dicarboxylic acid, Ald= aldrtithiol) has been synthesized through slow diffusion technique. Compound **1** is molecular structure and assembled through H-bonding forming a supramolecular architecture. The CuO_2N_3 units bridged through aldrithiol molecule to form the dimeric structure. The lattice water molecules are linked through H-bonding to form the decameric water cluster. The decameric water cluster are H-bonded to each other to form the 1D chain which resulted in excellent water stability and conduction of protons under humid condition. Band gap energy and magnetic measurements show that compound **1** is semiconductor and paramagnetic in nature. Further the compound is shown as a selective heterogeneous catalyst for styrene and cyclohexene epoxidation. This also shows facile oxygen reduction reaction (ORR) and can be used as a promising Pt-free cathode in alkaline Direct Methanol Fuel Cell (DMFC). The present results suggest that compound **1** is a promising multifunctional material.

Introduction

Design and construction of coordination polymers (CPs) or metal-organic frameworks (MOFs) with novel topologies and architectures has been motivated by their potential applications such as gas adsorption,[1] separation,[2] magnetism,[3] catalysis,[4] proton conductivity,[5] sensing[6] etc. CPs and MOFs are class of structures composed of organic ligand and inorganic building blocks. Most of these structures constituted with carboxylate based ligand. Structures containing carboxylate ligands are quite rigid. To render flexibility in the framework structure introduction of pyridyl linkers along with carboxylate ligands is one of the straight forward strategy.[7] Flexible structures are attractive due to their dynamic behaviour related with structural transformation.[8] Use of flexible ligands allow different bridging mode with the magnetically potent metal ions with variable distances and angles, which is responsible for interesting magnetic properties.[9] Among common hetero-acid pyridine based carboxylic acid generally prefer to form lower dimensional structures due to their preferred binding mode. The essential features of the lower dimensional structures are unsaturated coordination of the metal ion and crystallised with solvent molecules.[10] These solvents molecules are strongly H-bonded with the framework to form the supramolecular structures. These unsaturated coordination sites are potential sources for Lewis acid based catalysis.[11] Lewis acid catalyst often used for olefin epoxidation. Recently it has been reported that CPs or MOFs are ideal candidates for heterogeneous catalysis due to their chemical and thermal stability, accessible metal coordination sites and higher surface area.[12] Also, the hydrogen bonded network formed by solvents (coordinated or lattice) and oxygen atoms of linkers are found to favour proton transfer within such frameworks.[5] Proton conducting materials have become important for their role as electrolytes in fuel cells. In this regard, CPs or MOFs have been recently studied as potential proton conducting materials. Their hierarchal and designable structures, chemical functionalization of the pores and crystallinity facilitate targeted designing of the framework to bring about proton conduction.

MOF chemistry is very rich with applications like gas adsorption, gas separation, magnetism, catalysis, proton conductivity, sensing etc. and it has also seen that most of the cases these MOF exhibit single or related properties like gas adsorption and or gas separation and or magnetism. This is very rare where multiple properties has been studied in a particular CP or MOF.

Here we have synthesized a copper based coordination compound using 2, 4-pyridine dicarboxylic acid and aldrithiol ligand. The compound, $[Cu_2(PDA)_2(Ald)_2(H_2O)_2]$. $8H_2O$, **1**, contains two CuO_2N_3 units, which bridges by aldrithiol moiety to form the dimer structure. The structure is stabilized through extensive H-bonding and form the H-bonded layered structure. Lattice water molecules are H-bonded to form the decameric cluster, which are linked to form the one-dimensional water cluster chain. Band gap energy and magnetic measurements exhibit the semiconductor and paramagnetic behaviour. Compound **1** is shown as a selective heterogeneous catalyst for styrene and cyclohexene epoxidation. It shows oxygen reduction reaction (ORR) and can be used as a promising Pt-free cathode in alkaline Direct Methanol Fuel Cell. This compound demonstrate water stability and proton conductivity of 1.19×10^{-5} S cm^{-1} at 45 °C with 100 % relative humidity (RH). It is always interesting to have single compound with multiple functionality and the present results show compound **1** is a promising multifunctional material.

View Article Online
DOI: 10.1039/C6RA05961A

Results and discussion

Structural description

The single crystal X-ray diffraction data depicts that the compound **1** crystallizes in triclinic system with a space group of *P* (-1) (Table S1). The asymmetric unit contains one Cu ion, one PDA molecule, an aldrithiol molecule, one coordinated water molecule and four lattice water molecules. The Cu atom adopts distorted square pyramidal geometry with three nitrogen atoms (two from Ald and one from PDA) and two oxygen atoms (one from PDA anion and one from the coordinated water molecule). The CuO_2N_3 polyhedral units are linked through aldrithiol molecule to form the dimeric structure (Figure 1a). The deprotonated COO groups of the dimeric unit are H-bonded through coordinated water molecules to form the two-dimensional structure (Figure 1b).

Interestingly, compound **1** reveals interlayer hydrophilic 1D channels running parallel to the *b* axis, which are filled with lattice and coordinated waters (Figure S1). The hydrogen bonding association of lattice water molecules lead to the formation of decameric water cluster (Figure 1c).[13] In the decameric cluster, cyclic tetramer is formed by water molecules O(400) and O(500) and their symmetry-related counter parts, with O(100), O(200); and O(300) monomer dangling from O(400) and O(500), respectively. This water tape consists of novel water decamer with the geometry of noncoplanar cyclic structure. Adjacent decamers are fused together by sharing one edge formed by O(500) … O(500) with the separation of 2.853 Å, forming a one-dimensional water chain along the *c* axis. The O··· O distances vary from 2.488–2.960 Å with an average O··· O separation of 2.72 Å, compared to 2.85 Å in liquid water.[14] The data presented in Table S2 also suggest the hydrogen bonding interaction among the water molecules. Such highly ordered infinite one-dimensional water cluster consisting of fused water decamers is potential proton conducting pathway.

(a)

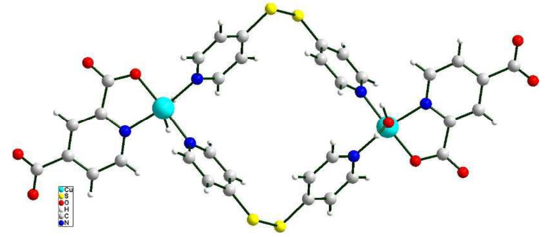

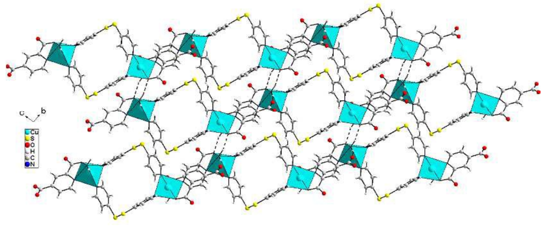

(b)

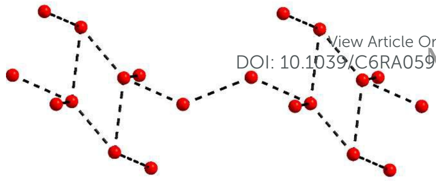

(c)

Fig. 1 (a) Copper dimer in **1**, (b) H-bonded layered structure of compound **1**, (c) Hydrogen bonding association of water molecules into extended one-dimensional chains.

Band Gap Energy

We have collected the diffuse reflectance UV-Vis spectra of the powder sample of **1** in order to measure the band gap energy (E_{bg}), which was confirmed as the intersection point between the energy axis and the line extrapolated from the linear portion of the adsorption edge in a plot of the Kubelka–Munk function *vs*. energy. As shown in figure S2a, the optical absorption associated with E_{bg} can be assessed at 2.24 eV for **1**. We also measured the optical band gap energy of Na-PDA and the value is 3.82 eV (Fig. S2b). We have measured the indirect band gap energy in this case as these types of inorganic-organic hybrid structures exhibit very small dispersion and flat valence band (VB) and conduction band (CB).[15] The carboxylate ligands on inorganic-organic hybrid structures determine the valence and conduction bands.[15] The optical band gap energy of **1** lesser compared to corresponding Na-salt of carboxylic acid is likely due to the distribution of charge at the interface between organic linker and metal ion in the coordination polymers.

Alkene oxidation

Catalytic abilities of compound **1** were studied by alkene oxidation. Styrene and cyclohexene were used as model substrate to identify the optimal reaction conditions in the presence of *tert*-butyl hydroperoxide (TBHP). Compound **1** exhibits good activities of alkene oxidation with reasonably good selectivity (Table 1). The control reaction without catalyst gave no reaction product.

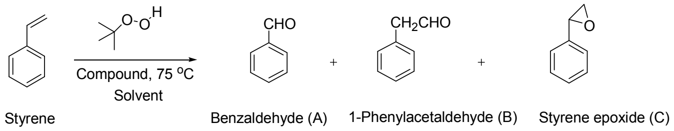

Scheme 1. Oxidation products of styrene

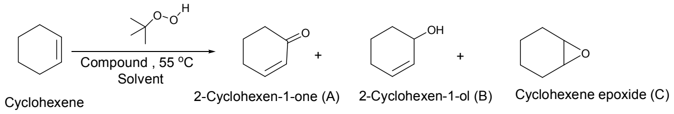

Scheme 2. Oxidation products of cyclohexene

Table 1. The oxidation of styrene and cyclohexene in the presence of TBHP, using **1** as catalyst.

Styrene oxidation[a]					
Solvent (temp)	Time (h)	Conversion (%)	Selectivity (%)		
			(A)	(B)	(C)
DCE (75 ˚C)	3	65	52	-	5

View Article Online
DOI: 10.1039/C6RA05961A

Cyclohexene oxidation[b]					
DCM (55 ºC)	3	65	46	-	-

[a] Reaction conditions: Substrate (1.74 mmol); TBHP (2 mmol); catalyst (0.03 mmol). (A) benzaldehyde; (B)1-Phenyl acetaldehyde, (C) styrene epoxide

[b] Reaction conditions: Substrate (1.97 mmol); TBHP (2 mmol); catalyst (0.03mmol). (A) 2-cyclohexen-1one; (B) 2-cyclohexen-1-ol; (C) cyclohexene epoxide.

Based on the literature it is predicted that copper metal ion activates TBHP, forming different types of intermediates (peroxometal, oxometal or free radicals). The products are benzaldehyde, 1-phenylacetaldehyde and styrene oxide with high selectivity for benzaldehyde and this is due to two step mechanism, starting with the attack of $(CH_3)_3O\dot{O}$ on styrene (Scheme S1).[16] Cyclohexene oxidation showed a high yield towards ketone, and complete absence of diols and epoxide. Most probably the TBHP activation occurs on the unsaturated surfaces of the compound **1** by a similar radical mechanism for the styrene oxidation (Scheme S2).[16] The catalyst (compound **1**) can be used up to third cycle without change of any significant structural integrity and yield (Fig. S3).

Magnetism

The molar magnetic susceptibility (χ_m) of the powder sample of **1** was measured in the temperature range 2-400 K (Fig. 2). The χ_m value increases as the temperature decreases following Curie Weiss (CW) behaviour, which shows the sample to be paramagnetic in nature. In order to extract the magnetic parameters, the high temperature data were analysed by fitting $\chi(T)$ in the following expression

$\chi_m = \chi_o + C/(T+\theta)$, where χ_o is the temperature independent susceptibility and the C is curie constant and θ is the characteristic CW temperature (Fig. S3). The data were fitted with parameters, $\chi_o \approx -1.73459\times10^{-4}$ cm^3/mol, $C \approx 0.52691$ cm^3 K/mol and θ (CW) $\approx$ 1.08467 K. From the value of C, the effective moment was calculated to be 2.05 μ_B from the equation $\mu_{eff} = \sqrt{}(3K_B C/N_a)$, where N_a is the Avagadro number and K_B is the Boltzman constant. This value is comparable to the spin-only value of $\mu_{eff} = g\sqrt{S(S+1)}\mu_B \approx 1.73$ μ_B for Cu^{+2} (S = 1/2) assuming g = 2. Since the value of θ is negligible, the interaction between the copper spins are considered to be very weak. The M *vs* H curve at 2.1 K shows (Inset Fig. 2) a linear increase at low fields and saturates at 8 T to a saturation magnetization $M_s \approx 1$ μ_B. For spin ½ systems the saturation magnetization is expected to be ($M_s = gS\mu_B$) 1 μ_B. The shape of the M vs H curve is similar to that of a paramagnetic curve.

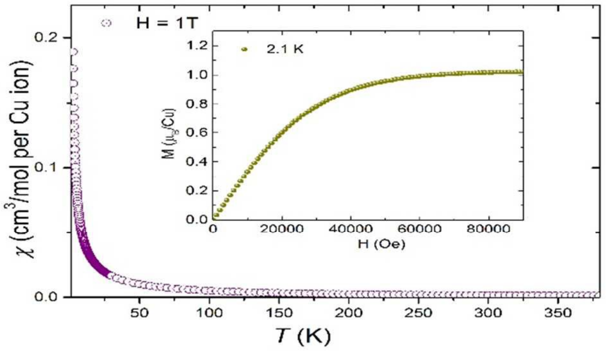

Fig. 2 Temperature variation of the molar magnetic susceptibility (χ_m) for **1**. The inset shows the corresponding magnetization (M) *vs* field (T) plot.

Oxygen Reduction Reaction

Non-platinum catalysts such as octabutylsulphonylphthalocyanine complexes of iron and cobalt supported on multi-walled carbon nanotubes (MWCNTs)[17a], graphene-metalloporphyrin composite[17b], iron tetrasulfophthalocyanine (FeTSPc) supported on single-walledcarbon nanotubes (SWCNTs)[17c] are explored as low cost alternatives to expensive platinum based catalysts for oxygen reduction reaction (ORR) in direct alcohol fuel cells (DAFCs). In comparison to the above mentioned metal macrocycles use of simple coordination compounds such as compound **1** (Cu-dimer) dispersed on Ketjenblack carbon (Cu-dimer/C) for ORR will further reduce the cost of the catalyst. Fig. S5 shows that cyclic voltammetry curves of Cu-dimer/C and ketjenblack carbon in N_2 saturated 0.1 N KOH solution recorded at 10 mV s^{-1} at room temperature. As shown in Fig. S5 a pair of broad peaks are observed between 0.6 V to 0.83 V *vs*. RHE, which is attributed to the redox transformation of Cu centres in Cu-dimer, which is believed to mediate the ORR. Fig. 3 depicts series of linear sweep voltammograms (LSVs) recorded for Cu-dimer/C in O_2 saturated 0.1 N KOH solution at a scan rate of 10 mV s^{-1} and at rotation rates of 200, 400, 600, 800, 1000, 1200, 1400 and 1600 rpm. With increase in rpm, the limiting current also increased indicating that ORR in 0.1 N KOH electrolyte is diffusion limited.

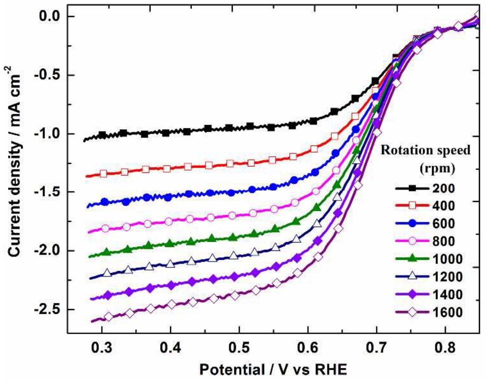

Fig. 3 LSV of Cu-dimer/C in O_2 saturated 0.1N KOH solution at different rotation speed.

Fig. 4a shows the polarization curve obtained from disk and chronoamperometry profile (measured at 0.55 V vs. RHE) obtained from the Pt ring of Cu-dimer/C coated rotating ring-disk electrode (RRDE). To quantitatively verify the ORR mechanism, Cu-dimer/C was characterized using RRDE study. The electron number (n) and hydrogen peroxide yield (% HO_2^-) during ORR can be determined using equations 3 and 4 respectively,

$$n = 4 * \frac{I_{disk}}{I_{disk} + \frac{I_{ring}}{N}} \quad (3)$$

$$\%\ _{HO_2^-} = \frac{{2I_{ring}}/{N}}{I_{disk} + {I_{ring}}/{N}} * 100 \quad (4)$$

Where N = 0.39, I_{disk} and I_{ring} denotes the collection efficiency, disk current and ring current respectively. If O_2 undergoes complete reduction into OH^- ions, n value would be 4 and the % HO_2^- would be zero. Since ORR is multistep process the n value involved in ORR can be derived from RRDE measurement. The intermediates of ORR such as HO_2^- can be detected by oxidizing at the ring. Employing the I_{disk} and I_{ring} values, corresponding n values calculated were found to be between 3.4 to 4.0 in the potential range of 0.3 to 0.8 V vs. RHE (Fig. 4b). In addition, Fig. 4b depicts the % HO_2^- generated during ORR. The trend in "n" and "% HO_2^-" were

View Article Online
DOI: 10.1039/C6RA05961A

strongly disk potential-dependent and maximum in % HO_2^- was about 23 % at around 0.37 V vs. RHE.

Figs. S6 and S7 show the LSVs recorded at 1600 rpm in O_2 saturated 0.1 M KOH solution, in the presence and absence of 1 M methanol for Cu-dimer/C and Pt/C catalyst respectively. ORR activity of Cu-dimer was shifted negatively about 43 mV at $E_{1/2}$, probably due to adsorption of methanol on the copper center, however there was no change in the ORR profile. In contrast, for Pt/C, in presence of methanol, ORR activity was completely masked with the methanol oxidation. Hence, we conclude that Cu-dimer/C could be employed as methanol tolerant ORR catalyst in DAFCs. Hence, Cu-dimer/C could be a potential low cost ORR catalyst for DAFCs.

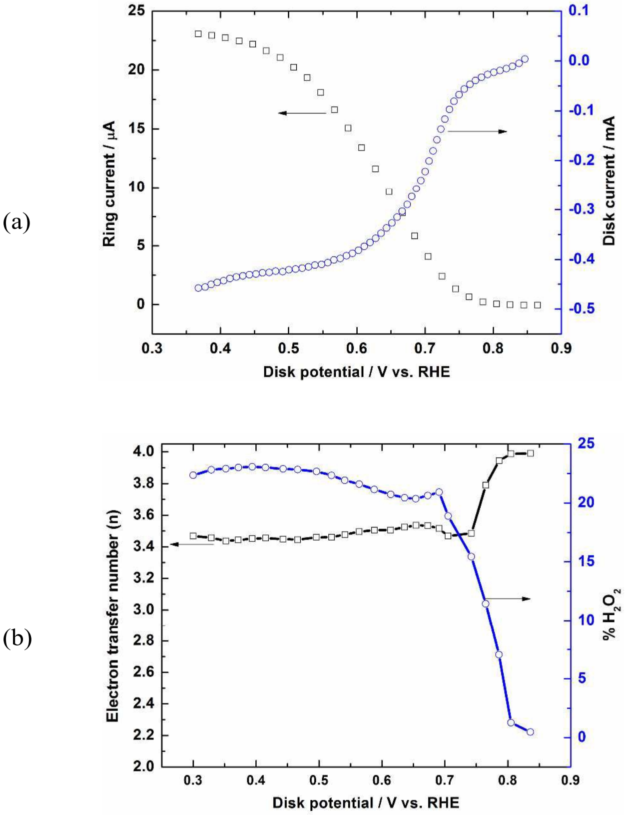

Fig. 4 RRDE study using Cu-dimer/C coated glassy carbon electrode in O_2-saturated 0.1 N KOH solution at a rotation speed of 1600 rpm shows the (a) disk and ring current profile and (b) the "% HO_2^-" generated and "n" as a function of disk potential.

Proton Conductivity

Considering the structure and the water stability, the proton conductivity of compound **1** is measured by using EIS technique and Nyquist plot, where impedance (Z*=Z'+iZ") of the complex is calculated as a function of relative humidity (RH) and temperature. The overall resistance (R) was obtained by extrapolating the semi-circular arc to the Z' axis at the low frequency side of the Nyquist plot. The conforming conductivity (σ) was calculated by: σ = d/RA, where d is the thickness and A is the area of the respective pellet.

The plots of log (σT) versus 1000/T is linear which can be fitted in the equation $T_\sigma = \sigma_0 \exp(-E_a/KT)$, where σ_0 is a pre exponential factor, E_a is activation energy, K is Boltzmann's constant and T is absolute temperature. The Nyquist plot in the form of a semicircle ending in a tail reflects the response at the electrode and the pellet interface. The conductivity of the pellet was found to vary between 10^{-6} to 10^{-5} S cm^{-1}, with increase in temperature from 25 ºC to 45 ºC at 100% RH (Fig. 5). Maximum conduction was attained at 45 ºC wherein conductivity was found to be 1.19×10^{-5} S cm^{-1} at 100 % RH, which is quite similar with respect to other coordination polymers.[5] The sample showed the activity till 45 ºC. The impedance plot nature was found to change abruptly on further increase in the temperature thereby reflecting its inability to conduct protons there onwards. The activation energy for the compound was found to be 0.16 eV from the Arrhenius plot (Fig. S8).

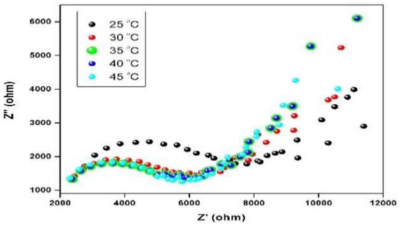

Fig. 5 Nyquist plot of **1** at 100% RH at various temperature.

It is always interesting to synthesize materials with multifunctional behavior. Due to Lewis acid character and variable oxidation state copper metal exhibit interesting catalytic and magnetic behavior. Here we have synthesized a lower dimensional coordination compound based on copper. The as-synthesized compound exhibit activity towards alkene epoxidation. Due to dimeric behavior of this complex the unpaired electrons are interacting each other in paramagnetic fashion. The unique structural features provoked us to explore the conductivity and Fuel cell application. The proton conductivity data is in the order of 10^{-5} S cm-^{1}. Fuel cell activity showed this compound can be used as methanol tolerant ORR catalyst for DAFCs. There are several copper based CPs or MOFs are reported with interesting magnetic properties or as a Lewis catalyst or as a good proton conductor or as cathode for DAFCs. The example of one compound with all the above said properties is very rare. The present compound exhibit all these properties but the activity is not in order of highest range. Presently we are working on to synthesize novel ligand which can be used for new CPs or MOFs with multifunctional properties in higher order of magnitude.

Experimental Section

Materials. All chemicals were of reagent-grade quality obtained from Sigma-Aldrich and used as received without further purification. The FT-IR spectrum was recorded from KBr pellets in the range of 4000-400 cm^{-1} on a Perkin-Elmer, SPECTRUM 1000 spectrometer. The TGA was performed on SDT Q600 (Shimadzu) analyser in flowing nitrogen with a heating rate of 10 ^{0}C per minute. Powder X-ray diffraction data were collected using an X'pert PRO (PANalytics) powder diffractometer equipped with Cu Kα radiation (1.540598 Å).

Synthesis

$Cu(NO_3)_2$. 2.5 H_2O (0.1 mmol, 23.2 mg) was dissolved in 10 mL of water. 2,4 pyridine dicarboxylic acid (0.1 mmol, 16.7 mg) was taken with 10 mL of water, maintaining a pH of 8 by adding 0.15 mmol NaOH followed by aldrithiol (0.1 mmol, 22 mg), dissolved in ethanol and stirred for 3 h. A buffer of EtOH and water mixture (1:1) were freshly prepared. Metal salt solution, buffer, ligand and co-ligand mixture (1:1:1) was added to a vial by layer by layer method. Deep blue coloured clear crystals were formed after 10 days

View Article Online
DOI: 10.1039/C6RA05961A

in room temperature. The crystals were washed and then dried for further use.

Single Crystal X-ray Diffraction. For single crystal XRD measurement, a suitable crystal was carefully selected under a polarizing microscope and glued to a thin glass fiber. The single crystal diffraction data were collected on a Bruker AXS Smart Apex CCD diffractometer at 298 K. The X-ray generator was operated at 50 kV and 35 mA using MoK_α (λ = 0.71073 Å) radiation. Data were collected with ω scan width of 0.3 °. A total of 606 frames were collected in three different settings of φ (0 °, 90 °, 180 °) keeping the sample to-detector distance fixed at 6.03 cm and the detector position (2θ) fixed at -25 °.

The data were reduced using SAINTPLUS[18] and an empirical absorption correction was applied using the SADABS program.[19] The crystal structure was determined by direct methods using SHELXS97 and refined using SHELXL97 present in the SHELXTL V6.14[20] package. The asymmetric unit contains four "uncoordinated" water molecules. The hydrogen atoms of all the water molecules (except O200) could not be located from a difference Fourier map. On account of this short O...O contacts were observed in the crystal structure. All other hydrogen atoms were placed in calculated positions during the final step of the refinement process. For the final refinement, the hydrogen atoms were placed in geometrically ideal positions and refined using the riding mode. The last cycles of the refinement included atomic positions, anisotropic thermal parameters for all the non-hydrogen atoms, and isotropic thermal parameters for all the hydrogen atoms. Full-matrix-least-squares structure refinement against F^2 was carried out using the WINGX[21] package of programs. The crystallographic parameters for compound **1** is provided in table S1. CCDC- 1433869 contains the crystallographic data for **1**. This data can be obtained free of charge from The Cambridge Crystallographic Data Centre (CCDC) via www.ccdc. cam.ac.uk/data_request/cif

Characterization

Initial characterization were carried out by powder X-ray diffraction (XRD), thermogravimetric analysis (TGA), and IR spectroscopic studies. The powder XRD pattern was recorded on crushed single crystals in the 2θ range 5-50 º. The XRD pattern indicated that the product was a new material; the pattern was entirely consistent with the simulated XRD patterns generated based on the structures determined using single-crystal XRD (Fig. S9). The TGA for as synthesized materials showed an initial weight-loss step at around 100 °C which is due to the loss of coordinated and lattice water molecules (Fig. S10).Compound **1** was stable up to 250 °C (Fig. S11). The second weight loss after 250 °C is due to loss of organic moieties. We have carried out the water stability of compound **1** by soaking the sample in water and it shows that compound **1** is stable in water even after **1** month without any loss of mass and structural integrity (Fig. S12). IR spectrum exhibited typical peaks corresponding to the lattice and coordinated water molecules, aldrithiol and carboxylate moieties in their respective bands (Fig. S13).

Optical Band-Gap Measurements

The optical absorption spectra of **1** and Na-salt of pyridine dicarboxylic acid were collected on a Shimadzu UV/Vis/NIR spectrophotometer. The room temperature diffuse reflectance spectra was measured using $BaSO_4$ as a reference material and converted to a Kubelka–Munk function, from which the band gap of the compound was estimated.[21,22] This two-flux model, which considers only diffuse light, is used to determine the absorption coefficient from a surface that both scatters and absorbs incident radiation. For a crystalline solid with a band gap (E_{bg}), the frequency dependence (ν) of the absorption coefficient (κ) can be approximated as

$$\kappa(v) = \frac{B_T\left(h\nu - E_{bg}\right)^n}{h\nu}$$

where B_T is a constant derived from the square of the averaged dipolar momentum matrix element and n is equal to 0.5 and 2 for direct and indirect band gap transitions, respectively.[23] The absorption coefficient (κ) can be measured from the reflectance (R) and expressed as $\kappa = (1 - R)^2/(2R)$. Using the above equation, the band gap of a material can be obtained by extrapolating to zero with the linear fit to a plot of $(kh\nu)^{1/n}$ *vs* hν.

Alkene oxidation

The heterogeneous oxidation reactions were performed in two necked round bottom flasks fitted to a condenser under nitrogen atmosphere. The optimum temperature obtained was 75 °C for styrene and 55 °C for cyclohexene. Appropriate amount of catalyst (16.27 mg, 0.03 mmol) was taken in 5 mL of dry solvent (dichloroethane for styrene and dichloromethane for cyclohexene) and heated till the optimum temperature was attained in each case. Then, substrate (0.2 mL for styrene (1.74 mmol), 0.176 mL for cyclohexene (1.74 mmol)) and the oxidant (0.192 mL (2 mmol) 70% TBHP in water) were added and stirred continuously. The molar ratio of substrate: oxidant: catalyst (58: 66: 1) was studied. Aliquots (1μL) was inserted and analysed by gas chromatography.

Gas chromatography was carried out in GC-MS QP2010 PLUS which is well equipped by secondary electron multiplier with conversion dyanode and a capillary column Rtx-1MS (30 m × 0.25 mm × 0.25 μm). Helium was used as a carrier gas. By using standard compounds, the products were recognised by GC-MS.

Magnetic Measurements

The magnetic properties were measured using a vibrating sample magnetometer (VSM) attachment in a commercial (Quantum Design) physical property measurement system (PPMS). Magnetic susceptibility χ as a function of temperature (T) was measured at different applied fields and over a large *T*-range (2 K ≤ T ≤ 380 K). Zero-field-cooled (ZFC) and field cooled (FC) magnetic susceptibilities were measured at an applied field of 0.05 T and at low temperatures. Magnetization isotherm (magnetization M vs. applied field H) was also measured at *T* = 2.1 K up to a maximum varying field of 9 T.

Electrochemical Characterization

10 mg of compound **1** and 10 mg of Ketjenblack carbon and 10 μL of 5 wt.% Nafion solution was added in 2 mL of water and 1 mL of isopropyl alcohol mixture and sonicated for 1 h to obtain a homogeneous ink. This ink was drop casted on to the 5 mm diameter glassy carbon rotating disk electrode (RDE, Pine Instruments) to obtain a Cu dimer loading of 200 $\mu g cm^{-2}$. 10 μL of diluted Nafion solution was drop-coated on the catalyst layer to protect it from falling off from the glassy carbon (GC) electrode. This electrode was subjected to cyclic voltammetry (CV) in aqueous 0.1 N KOH solution saturated with N_2 gas. Herein after, the Cu dimer mixed with Ketjenblack carbon is called as Cu-dimer/C. Similarly Cu-dimer/C coated glassy carbon based rotating ring disk electrode (RRDE, Pine Instruments, USA) were used to study the mechanism of ORR in oxygen saturated 0.1 N KOH solution. The electron transfer number (n) and the fraction of hydrogen peroxide generated during the ORR were evaluated using the disk and ring currents

View Article Online
DOI: 10.1039/C6RA05961A

obtained from RRDE study. To study the methanol tolerance behaviour of the catalyst, ORR was performed in 0.1 N KOH solution containing 1 M methanol. A Biologic VSP Model potentiostat was employed for electrochemical studies. A three electrode glass cell containing catalyst coated RDE/RRDE, a Hg/HgO, 0.1N aq. KOH reference electrode and carbon felt counter electrode was used for electrochemical studies. Potential measured against Hg/HgO, 0.1 N KOH electrode was converted into reversible hydrogen electrode scale (RHE). Instead of platinum based counter electrode, carbon felt was chosen to avoid contamination of the working electrode with platinum during electrochemical measurement.

Impedance Analysis

The alternating current (AC) impedance measurements were carried out by two electrode probe configuration set up, using BioLogic VPM3 electrochemical work station connected to a temperature controllable incubator (SH-241, ESPEC Co. Ltd., Japan). Compound **1** was finely grounded and then evacuated at 100 ºC under vacuum. The evacuated powder was then pressed to a pellet using a standard die (13 mm diameter). The incubator was initially flushed with N_2 before the measurements to remove moisture. The pellet was heated slowly and held at desired temperature for ~ 1 h before the analysis, to attain saturation. The pellet was subjected then to AC impedance analysis and the frequency was swept in the range of 1MHz−100Hz and 10 mV input voltage amplitude. The resistance was calculated by fitting the semicircle of the Nyquist plot. The activation energy was determined from the slope of Arrhenius plot.

Conclusions

We have synthesized a new coordination polymer, $[Cu_2(PDA)_2(Ald)_2(H_2O)_2]$. $8H_2O$, **1**, using solvent diffusion technique. Compound **1** exhibit interesting structural features, water and thermal stability. The presence of one-dimensional water cluster chain with decameric water cluster is noteworthy. The optical absorption associated with band gap measurements show this compound is semiconductor in nature. The magnetic measurements exhibit the paramagnetic behaviour. Further the compound is shown as a selective recyclable heterogeneous catalyst for styrene and cyclohexene oxidation. Compound **1** shows facile oxygen reduction reaction (ORR) and can be used a promising Pt-free cathode in alkaline Direct Methanol Fuel Cell (DMFC). Compound **1** also demonstrates potential proton conductivity because of the presence of water cluster chain, which is appropriate pathways for proton transporting. These results may encourage researchers to explore new multifunctional coordination polymers for proton transporting and alternating cathode for Pt-free DMFC.

Acknowledgements

We acknowledge financial support from Council of Scientific Research (CSIR), Govt. of India, through a grant 01(2778)/14/EMR-II. We are grateful to Prof. V. Ramakrishnan for encouragement and N. Ahmed for the help regarding magnetic measurements.

Notes and references

[a] School of Chemistry
Indian Institute of Science Education and Research Thiruvananthapuram,
Kerala, India-695016
Fax: (+91) 471-2597-438
E-mail: sukhendu@iisertvm.ac.in
Homepage: http://iisertvm.ac.in/~sukhendum

[b] Physical and Materials Chemistry Division, CSIR-National Chemical Laboratory (NCL), Pune, 411008, India

[c] Academy of Scientific and Innovative Research (AcSIR), New Delhi, India.

[d] Department of Chemistry, Indian Institute of Technology Madras, Chennai, 600036, India

Electronic Supplementary Information (ESI) available: Crystallographic parameters, H-bond tables, schemes for catalysis products, figures for band gap energy, recyclability of the catalyst, additional figure for magnetic and ORR measurements, PXRD, TGA and IR. See DOI: 10.1039/b000000x/

1 S. M. Cohen, *Chem. Rev*., 2012, **112**, 970.
2 N. Stock and S. Biswas, *Chem. Rev*., 2012, **112**, 933.
3 M. Kurmoo, Chem. Soc. Rev., 2009, 38, 1353.
4 a) Z. Xie, L. Ma, K. E. deKrafft, A. Jin, W. Lin, *J. Am. Chem. Soc.*, 2009, **132**, 922; b) M. Yoon, R. Srirambalaji, K. Kim, *Chem. Rev*., 2012,**112**, 1196; c) A. Dhakshinamoorthy, M. Alvaro, A. Corma, H. Garcia, *Dalton Trans.*, 2011, **40**, 6344.
5 a) P. Ramaswamy, N. E. Wong, G. K. H. Shimizu, *Chem. Soc. Rev.* **2014**, *43*, 5913; b) M. Yoon, K. Suh, S. Natarajan, K. Kim, *Angew. Chem. Int. Ed.* **2013**, *52*, 2688.
6 Z. Hu, B. J. Deibert, J. Li, *Chem. Soc. Rev.* **2014**, *43*, 5815.
7 (a) S. R. Ahrenholtz, C. Landaverde-Alvarado, M. Whiting, S. Lin, C. Slebodnick, E. Marand, A. J. Morris. *Inorg. Chem.* 2015, **54**, 4328; (b) C. Wang, F. Sun, K. Zhnag, C. Zheng, *Inorg. Chem. Commun.* 2014, **48**, 65; (c) X-M. Wang, R-Q. Fan, L-S. Qiang, P. Wang, Y-L. Yang, Y-L. Wang, *Dalton Trans.* 2014, **43**, 16152; (d) J. Xu, W. P. Su, M. C. Hong, *Cryst. Growth Des.* 2011, **11**, 337.
8 (a) S. Sanda, S. Goswami, H. S. Jena, S. Parshamoni, S. Konar, *Cryst. Eng. Commu.* 2014, **16**, 4742; (b) S. Sanda, S. Parshamoni, S. Konar, *Inorg. Chem.* 2013, **52**, 12866.
9 (a) B. K. Tripuramallu, S. Mukherjee, S. K. Das, *Cryst. Growth Des.* 2012, **12**, 5579; (b) B. K. Tripuramallu, S. K. Das, *Cryst. Growth Des* 2013, **13**, 2426.
10 R. Ghosh, K. S. Asha, S. M. Pratik, A. Dutta, R. Nath, S. Mandal, *RSC Advances* 2014, **4**, 21195.
11 J. Liu, L. Chen, H. Cui, J. Zhang, L. Zhang, C-Y. Su, *Chem. Soc. Rev.* 2014, **43**, 6011.
12 (a)Y. Qi, Y. Luan, J. Yu, X. Peng, G. Wang, *Chem. Eur. J.* 2015, **21**, 1589; (b) A. Dhakshinamoorthy, M. Alvaro, H. Garcia, *J. Catal.* 2012, **289**, 259.
13 a) L.-L. Han, T.-P. Hu, J.-S. Chen, Z.-H. Li, X.-P. Wang, Y.-Q. Zhao, X.-Y. Li, D. Sun, *Dalton Trans.* 2014, **43**, 8774; b) L. Infantes, J. Chisholm, S. Motherwell, *Cryst. Engg. Commun.* 2003, **5**, 480; c) L. Infantes, S. Motherwell, *Cryst. Engg. Commun.* 2002, **4**, 454.
14 a) B.-Q. Ma, H.-L. Sun, S. Gao, *Chem. Commun.* 2004, 2220; b) K. Liu, M. G. Brown, J. D. Cruzan, R. J. Saykally, *Science* 1996, **271**, 62; c) A. H. Narten, W. E. Thiessen, L. Blum, *Science* 1982, **217**, 1033.
15 a) C-K. Lin, D. Zhao, W-Y. Gao, Z. Yang, J. Ye, T. Xu, Q. Ge, S.

View Article Online
DOI: 10.1039/C6RA05961A

Ma, D-J. Liu, *Inorg. Chem.* 2012, **51**, 9039; b) C. H. Hendon, D. Tiana, M. Fontecave, C. Sanchez, L. D'arras, C. Sassoye, L. Rozes, C. Mellot-Draznieks, A. Walsh, *J. Am. Chem. Soc.* 2013, **135**, 10942; c) K. S. Asha, A. C. Reber, A. F. Pedicini, S. N. Khanna, S. Mandal, *Eur. J. Inorg. Chem.* 2015, **12**, 2085; d) K. S. Asha, P. R. Kavyasree, A. George, S. Mandal. *Dalton Trans.* 2015, **44**, 1009.

16 a) P. Cancino, V. Paredes-Garcia, P. Aguirre, E. Spodine, *Catal. Sci. Technol.* 2014, **4**, 2599; b) R. Ghosh, Y. C. Son, V. D. Makwana, S. L. Suib, *J. Catal.* 2004, **224**, 288; c) M. Silva, C. Freire, B. de Castro, J. L. Figueiredo, *J. Mol. Catal. A: Chem.*, 2006, **258**, 327.

17 a) S. A. Mamuru,K. I. Ozoemena, T. Fukuda, *Electrochim Acta* 2010, **55**, 6367; b) M. Jahan,Q. Bao,K. P. Loh, *J. Am. Chem. Soc*, 2012, **134**, 6707; c) G. Mo,S. Liao,Y. Zhang, *Electrochim Acta*, 2012, **76**, 430.

18 SMART (V 5.628), SAINT (V 6.45a), XPREP, SHELXTL; Bruker AXS Inc.: Madison, WI, 2004.

19 G. M. Sheldrick, Siemens Area Correction Absorption Correction Program; University of Göttingen: Göttingen, Germany, 1994.

20 G. M. Sheldrick, SHELXL-97 Program for Crystal Structure Solution and Refinement; University of Göttingen: Göttingen, Germany, 1997.

21 J. L Farrugia, *J. App. Crystallography*. 1999, **32**, 837.

22 (a) P. Kubelka, *J. Opt. Soc. Am.* 1948, **38**, 448, (b) P. Kubelka, *J. Opt. Soc. Am,* 1954, **44**, 330, (c) A. B. Murphy, *J. Phys. D: Appl. Phys.* 2006, **39,** 3571.

23 N. Laidani, R. Bartali, G. Gottardi, M. Anderle, *J. Phys.: Condens. Matter* 2008, **20**, 015216.